

A simple way to improve AVO approximations

Charles P. Ursenbach

ABSTRACT

Some twenty years ago it was suggested that the average angle, $\theta = (\theta_1 + \theta_2)/2$, in the Aki-Richards approximation could itself be approximated by the angle of incidence, θ_1 . The newly updated CREWES Reflectivity Explorer is a useful tool for exploring such questions. Using this tool, some numerical observations are described which suggest that approximating θ by θ_1 actually increases the accuracy of the theory at low angles (although the θ formulation is still superior near the critical angle). A theoretical study is outlined which is successful in explaining this interesting result. The theoretical study also suggests a means by which the strengths of both the θ and θ_1 formulations may be combined into one theory. This new theory is given, and is shown to be accurate over a wider range of angles than the θ_1 formulation. It is therefore promising for use with pre-critical AVO studies. The same approach can be applied to various derivatives of the Aki-Richards approximation, such as the Fatti and Smith-Gidlow approximations.

INTRODUCTION

The Zoeppritz equations (see Aki and Richards, 1980, pp 149-151) are well-known to give the reflection and transmission coefficients of P and SV plane waves at an interface. These are complicated expressions and, while suitable for AVO modeling, simplifications of them have been found useful for AVO inversion. The best known is the Aki-Richards approximation (Aki and Richards, 1980, pp 153-154), which is linearized in the following quantities:

$$\begin{aligned} R_\alpha &\equiv \frac{\alpha_2 - \alpha_1}{\alpha_1 + \alpha_2} \left(= \frac{1}{2} \frac{\Delta\alpha}{\alpha} \right) \\ R_\beta &\equiv \frac{\beta_2 - \beta_1}{\beta_1 + \beta_2} \left(= \frac{1}{2} \frac{\Delta\beta}{\beta} \right) \\ R_\rho &\equiv \frac{\rho_2 - \rho_1}{\rho_1 + \rho_2} \left(= \frac{1}{2} \frac{\Delta\rho}{\rho} \right) \end{aligned} \quad (1)$$

where α , β , and ρ are the P-wave velocity, S-wave velocity, and density, and subscripts 1 and 2 refer to the media above and below the interface. The R_i quantities are referred to as reflectivities, and the $\Delta x/x$ quantities are referred to as relative contrasts, being the ratio of the difference across the interface and the average across the interface. These three ratios, together with

$$\gamma \equiv \frac{\beta_1 + \beta_2}{\alpha_1 + \alpha_2} \quad (2)$$

and the angle of incidence define both the sixteen Zoeppritz coefficients and their Aki-Richards approximations. The two Aki-Richards approximations of most interest in exploration seismology can be written as

$$\begin{aligned} R_{PP}^{A-R} &= R_\rho + \frac{R_\alpha}{\cos^2 \theta} - 4\gamma^2 \sin^2 \theta (2R_\beta + R_\rho), \\ R_{PS}^{A-R} &= -\gamma \tan \varphi \left[R_\rho + 2\gamma \cos(\theta - \varphi) (2R_\beta + R_\rho) \right], \end{aligned} \quad (3)$$

$$\theta = (\theta_1 + \theta_2)/2, \quad \varphi = (\varphi_1 + \varphi_2)/2$$

where the linear dependence on the reflectivities is apparent.

Shuey (1985) rearranged R_{PP}^{A-R} of equation (3) into three terms with increasing powers of $\sin \theta$. A similar exercise can be carried out with R_{PS}^{A-R} and together these yield

$$\begin{aligned} R_{PP}^{Shuey} &= (R_\rho + R_\alpha) + \left[R_\alpha - 4\gamma^2 (2R_\beta + R_\rho) \right] \sin^2 \theta + \sin^2 \theta \tan^2 \theta R_\alpha \\ &\equiv A + B \sin^2 \theta + C \sin^2 \theta \tan^2 \theta, \\ R_{PS}^{Shuey-like} &= -\gamma \left[R_\rho + 2\gamma (2R_\beta + R_\rho) \right] \sin \theta + O(\sin^3 \theta) \\ &\equiv A_s \sin \theta + O(\sin^3 \theta). \end{aligned} \quad (4)$$

He then notes that, in practical applications between 0° and 30° , the incident angle θ_1 can be used in place of the average angle θ in equation (4). The resulting approximation is much less accurate near the critical point. However, it is shown below that it can, for low angles, not only be equally as accurate as the original Aki-Richards approximation, but can in fact yield results superior to those of equation (4)*. It is also shown that a theoretical explanation exists for this observation. Furthermore, this understanding can be used as a basis for the simple method of improving PP and PS AVO approximations.

EMPIRICAL OBSERVATIONS

A few years ago, CREWES introduced the Reflectivity Explorer. This Java applet is similar to the better known Zoeppritz Explorer (see “Explorer Programs” link at www.crewes.org), but is designed specifically to explore a variety of AVO-related approximations to the Zoeppritz R_{PP} and R_{PS} coefficients. It is thus an ideal tool for investigating the claims raised in the Introduction. An updated version of the Reflectivity Explorer was recently introduced, and it includes various forms of the Aki-Richards approximations, including the θ -dependent form (which is equivalent to the three-term Shuey approximation) and the θ_1 -dependent form.

A comparison of both approximations with the original Zoeppritz theory is shown in the applet output in Figure 1. This is a Class I AVO model with a critical angle of 48.59° . Figure 2 shows the parameters entered into the Explorer’s control panel. From Figure 1 it

* This effect may have been noted previously, but the author has been unable to find reference to it in the literature. If such a reference exists, he would appreciate it being brought to his attention.

appears that the θ -dependent theory matches Zoeppritz more accurately, particularly as one approaches the critical angle. After the critical angle, θ_2 becomes complex, and is given by

$$\theta_2 = \frac{\pi}{2} + i \cosh^{-1} \left(\frac{\alpha_2}{\alpha_1} \sin \theta_1 \right), \quad (5)$$

as shown in Appendix A. Thus $\theta = (\theta_1 + \theta_2)/2$ is complex as well. This is why the θ -expression has a critical angle, while the θ_1 -expression does not.

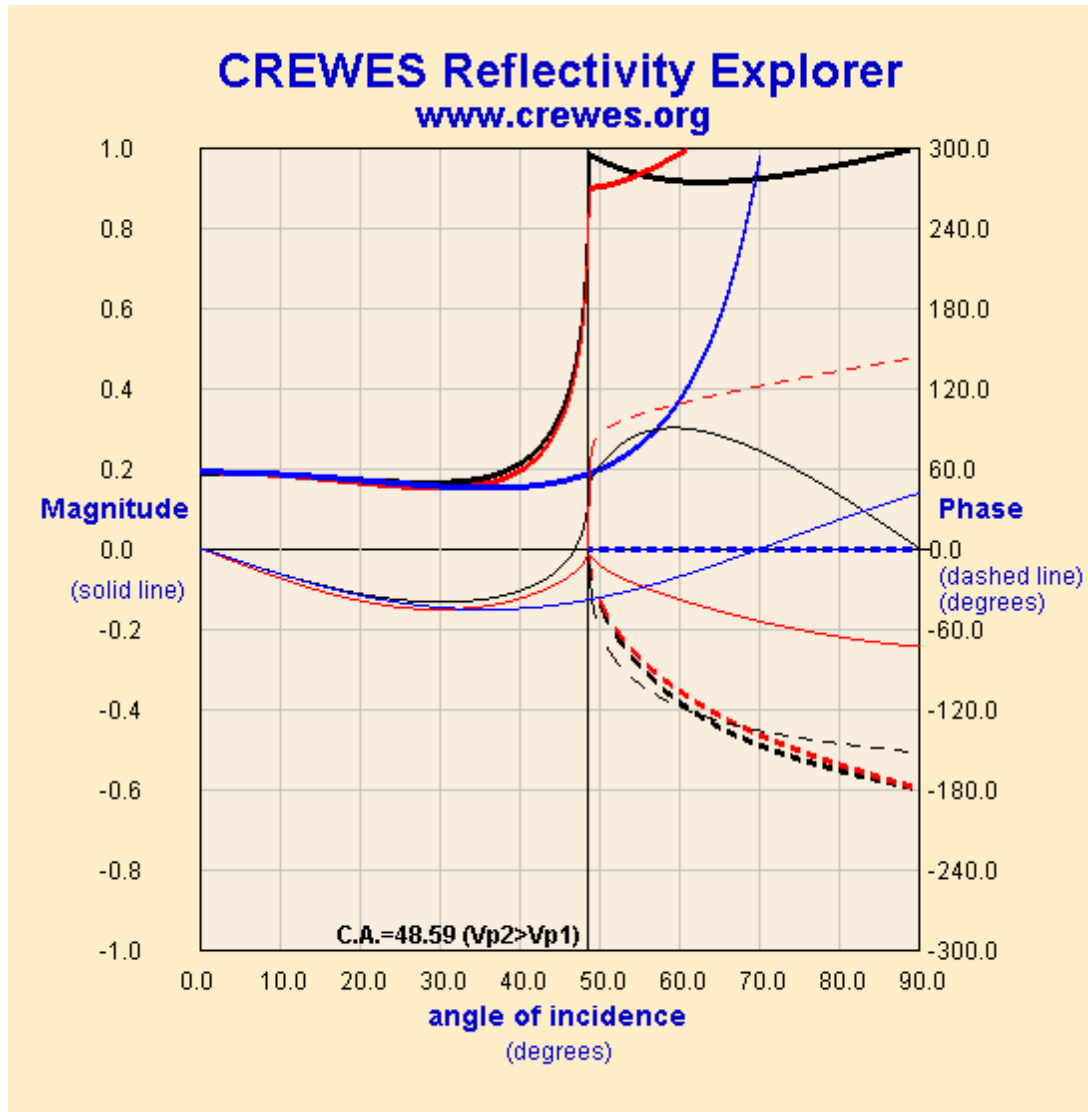


FIG. 1. The graphical output of the CREWES Reflectivity Explorer displaying R_{PP} and R_{PS} for parameters specified in Figure 2 (below). The θ -dependent approximation (red) appears to describe the Zoeppritz results (black) more accurately than the θ_1 -approximation (blue), particularly when approaching the critical angle at 48.59°.

Rpp (thick lines) Rps (thin lines)

Upper layer properties:

Upper layer density (ρ_1): kg/m³

Upper layer Vp (α_1): m/s

$(\beta_1 + \beta_2) / (\alpha_1 + \alpha_2)$:

Lower layer properties:

$\Delta\rho / \rho$:

$\Delta\alpha / \alpha$:

$\Delta\beta / \beta$:

Zoeppritz-Knott Aki-Richards(p)

Aki-Richards(theta) Aki-Richards(theta1)

Smith-Gidlow / Stewart Fatti / Larsen 2-term

New expression Elastic Impedance

Bortfeld Quadratic-Shear

Sine-squared of incidence angle:

Magnitude limits:

Phase limits (integers):

Display magnitude (solid) Display phase (dashed)

[Click here to recalculate graph](#)

Units: m/s and kg/m³ ft/s and g/cm³

FIG. 2. A screen capture of the Reflectivity Explorer control panel showing the parameters employed to obtain Figure 1 (above). Note that the lower layer properties have been replaced with relative contrasts defined in equation 1.

However, considering the lower angles in detail yields different conclusions. Figure 3 shows the detail for R_{PP} and Figure 4 the detail for R_{PS} . It is clear in both cases that the initial slopes are more accurately described by the θ_1 -dependent approximation.

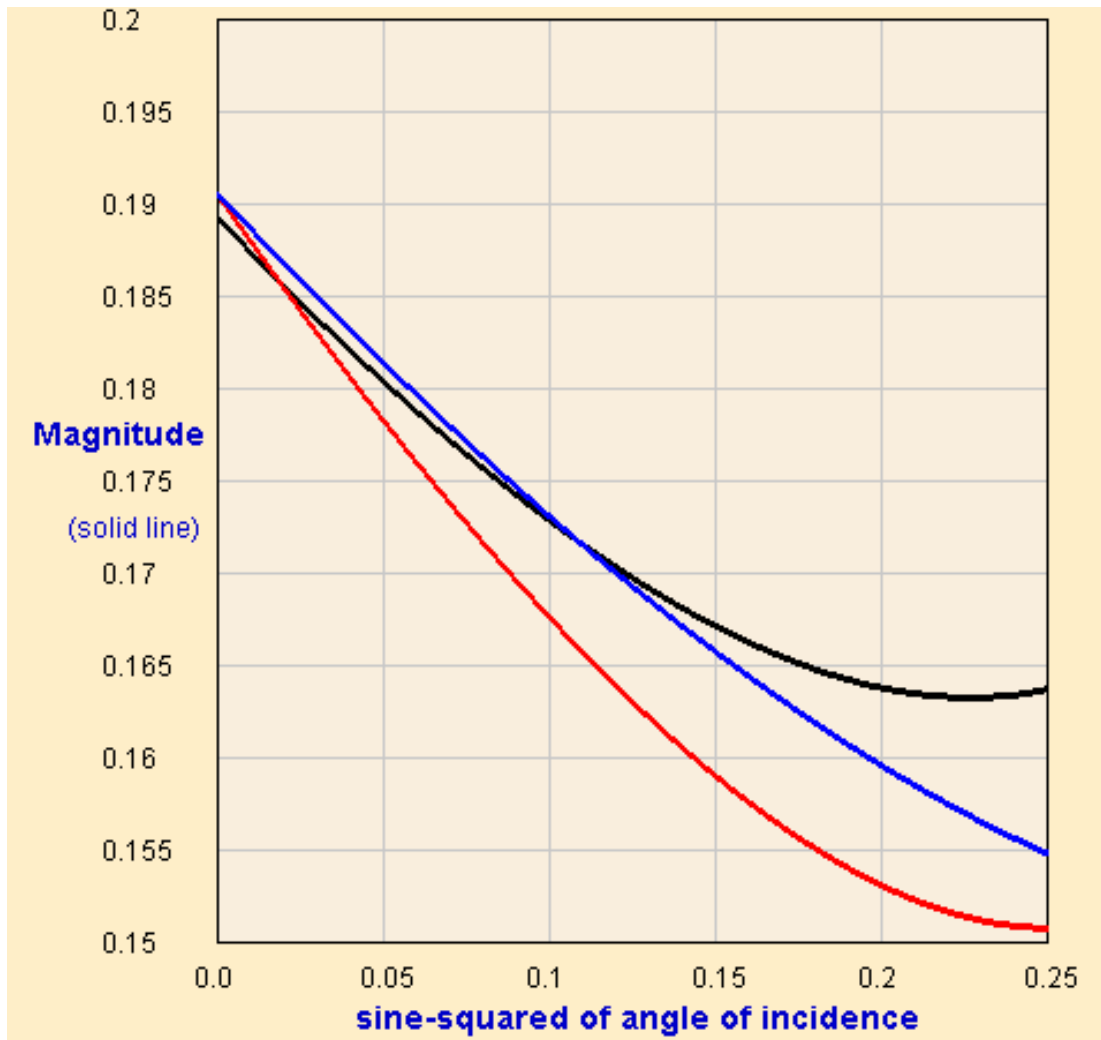


FIG. 3. A detailed view of $R_{PP}(\theta)$ with the same earth parameters as in Figures 1 and 2, but displaying only up to 30° . Note that the abscissa has been changed from θ_1 to $\sin^2\theta_1$ so that the behavior near $\theta_1 = 0$ is linear rather than quadratic. The θ_1 -expression (blue) is clearly a better approximation than the θ -expression (red) at low angle. (The exact Zoeppritz comparison is shown in black.).

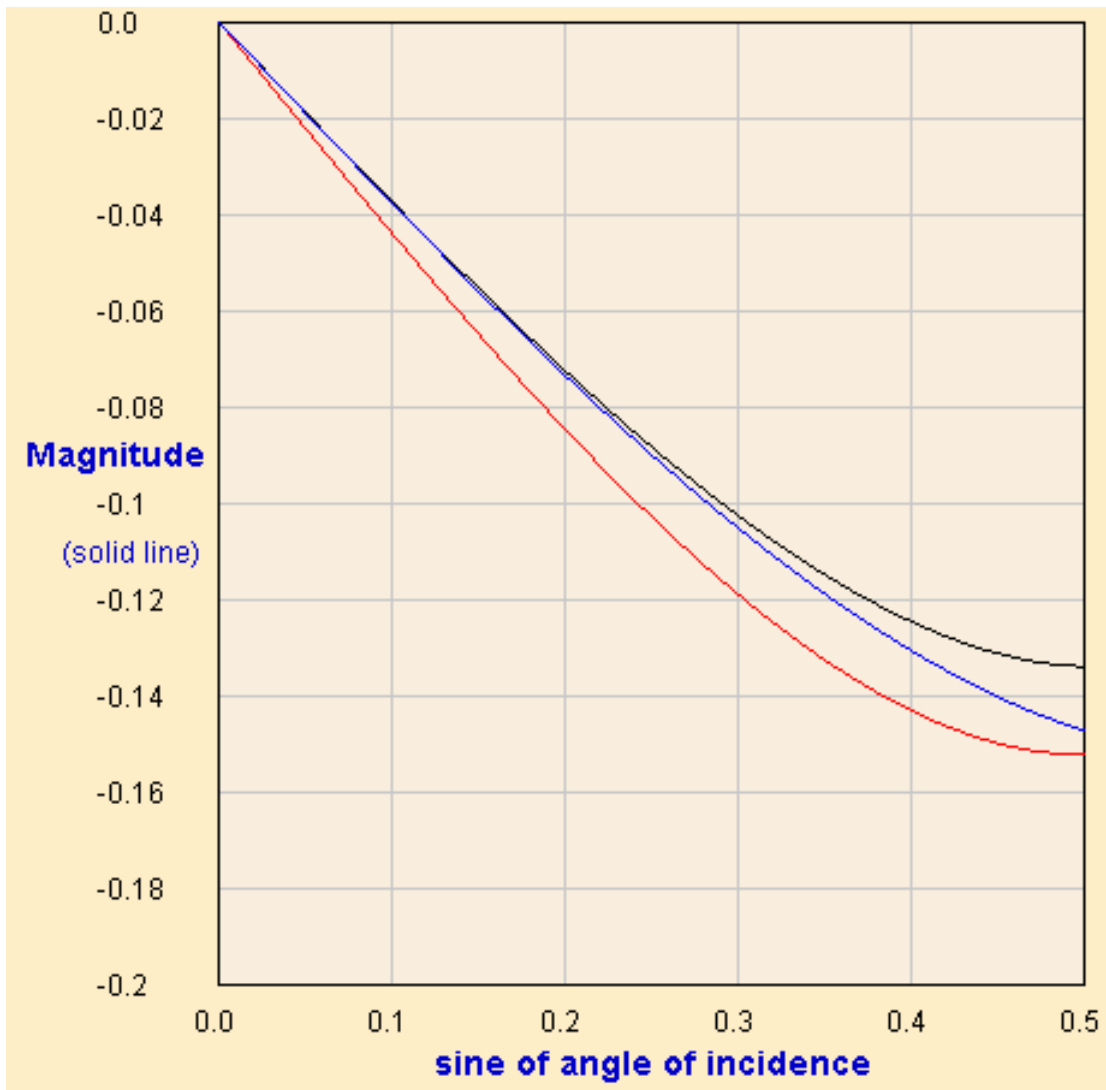


FIG. 4. A detailed view of $R_{pS}(\theta)$ with the same earth parameters as in Figures 1 and 2, but displaying only up to 30° . Note that the abscissa has been changed from θ_1 to $\sin\theta_1$, but both of these behave linearly near $\theta_1 = 0$, and are very similar over this range. The θ_1 -expression (blue) is clearly a better approximation than the θ -expression (red) at low angle. (The exact Zoeppritz comparison is shown in black.).

Figures 1-4 display results for only one set of earth parameters, so it is important to know if these results hold generally. The reader can easily put this to the test by accessing the Reflectivity Explorer on the software release accompanying this Research Report. No installation is required; the application is simply run by opening **REcrewes.html** or **REtest.html** in a browser window. The following points can then be verified:

- $R_{PS}(\theta_1)$ is more accurate than $R_{PS}(\theta)$ at low angles for virtually all earth parameter selections.
- $R_{PP}(\theta_1)$ is more accurate than $R_{PP}(\theta)$ at low angles for earth parameter selections roughly satisfying the mudrock trend (i.e., for which R_α and R_β possess the same sign and $|R_\beta| \geq |R_\alpha|$), and for which $\gamma \geq 0.35$. Violating either of these conditions leads to regimes where $R_{PP}(\theta)$ is more accurate than $R_{PP}(\theta_1)$, as shown in Figure 5. The value of R_ρ however does not appear to affect the accuracy much.
- Differences between θ_1 and θ formulations vanish at low angles for $R_\alpha = 0$. This is true for both R_{PP} and R_{PS} . There is no similar sensitivity, however, to R_β , R_ρ , and γ .

With these empirical observations in mind, we now turn to a theoretical analysis.

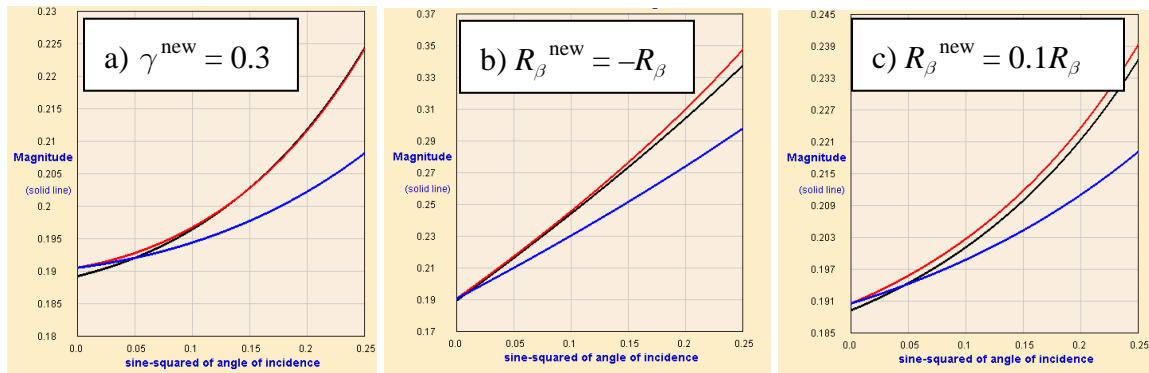


FIG. 5. Plots of R_{PP} for the same parameters as shown in Figure 2 except that in a) γ is set to 0.3, in b) R_β (or $\Delta\beta/\beta$) has its sign reversed, and in c) R_β is reduced by an order of magnitude. Comparing these with Figure 3 shows how changing γ and R_β can reverse the order of accuracy of $R_{PP}(\theta_1)$ and $R_{PP}(\theta)$.

THEORETICAL EXPLANATION

To find a theoretical explanation of our observations, we begin with the Zoeppritz equations. A standard reference (free of the typographical errors which plague many references) is Aki and Richards (1980, pp 149-151). These give the coefficients in terms of $\alpha_1, \beta_1, \rho_1, \alpha_2, \beta_2$, and ρ_2 . However there is redundant information in these six parameters, and the coefficients may be equivalently specified by the four ratios $R_\alpha, R_\beta, R_\rho$, and γ . For theoretical work and development of approximations it would be convenient to have the exact Zoeppritz coefficients expressed in terms of these ratios. Such expressions have been used in the past by the author, and for convenience they are given in this report in Appendix B. It is straightforward to encode the expressions in Appendix B into a symbolic mathematics program, such as MAPLE, and to then manipulate them in various ways.

We are interested investigating the differences in initial slopes (B and A_S from equation 4) for the θ and θ_1 formulations. We have noted that these differences vanish for $R_\alpha = 0$. To pursue this we apply a Taylor expansion in $\sin \theta_1$ to the exact Zoeppritz coefficients to obtain exact nonlinear analogues of B and A_S . (For completeness, the exact expressions for A, B , and A_S are given in Appendix C.) We then apply a second Taylor expansion to linearize these results in R_β and R_ρ . We do not linearize in R_α as the differences we are studying vanish for $R_\alpha = 0$, and so we wish to explore in greater detail the behavior with respect to this variable. The result of these manipulations yields

$$\begin{aligned}
 B^{\theta_1} &= [R_\alpha - 4\gamma^2(2R_\beta + R_\rho) - 2R_\rho R_\alpha^2] \frac{1 + R_\alpha}{1 - R_\alpha} \\
 B^\theta &= [R_\alpha - 4\gamma^2(2R_\beta + R_\rho) - 2R_\rho R_\alpha^2] (1 - R_\alpha^2) \\
 A_S^{\theta_1} &= -[R_\rho + 2\gamma(2R_\beta + R_\rho) - 2R_\rho R_\alpha] \\
 A_S^\theta &= -[R_\rho + 2\gamma(2R_\beta + R_\rho) - 2R_\rho R_\alpha] (1 + R_\alpha)
 \end{aligned} \tag{6}$$

The quantities in square brackets in equation 6 contain all of the linear terms of equation 4, plus each contains a nonlinear term as well. For a number of reasons we will assume that this non-linear term does not play a significant role in differentiating between the two theories. The first reason is that this term should be small for typical earth parameters. Secondly, the terms are identical in both B expressions and in both A_S expressions, and thus provide no ability to discriminate between the two methods. Thirdly, if these terms were key then the differences should vanish for $R_\rho = 0$, whereas they only vanish for $R_\alpha = 0$. Fourthly, we will show that we are able to find a completely satisfactory explanation of the differences without reference to them. Therefore we eliminate these terms, yielding equation 7:

$$\begin{aligned}
 B^{\theta_1} &= [R_\alpha - 4\gamma^2(2R_\beta + R_\rho)] \frac{1+R_\alpha}{1-R_\alpha} \\
 B^\theta &= [R_\alpha - 4\gamma^2(2R_\beta + R_\rho)](1-R_\alpha^2) \\
 A_S^{\theta_1} &= -[R_\rho + 2\gamma(2R_\beta + R_\rho)] \\
 A_S^\theta &= -[R_\rho + 2\gamma(2R_\beta + R_\rho)](1-R_\alpha)
 \end{aligned} \tag{7}$$

Now the non-linearity is expressed in solely through overall factors, and we note that $B^\theta / B^{\theta_1} = (1-R_\alpha)^2$ and $A_S^\theta / A_S^{\theta_1} = (1-R_\alpha)$. Since $R_{PP}(\theta) = R_{PP}(\theta_1)$ and $R_{PS}(\theta) = R_{PS}(\theta_1)$, this implies that

$$\frac{\sin \theta_1}{\sin \theta} = 1 - R_\alpha \tag{8}$$

to first order. This result is reasonable and agrees to first order with the exact relation,

$$\sin \theta_1 = \sin \theta \frac{1-R_\alpha}{\sqrt{1+R_\alpha^2 \tan^2 \theta}}, \tag{9}$$

which is derived in Appendix D. This leads to a straightforward explanation of the observations regarding R_{PS} . $R_{PS}(\theta_1)$ clearly has the correct slope, while $R_{PS}(\theta)$ has an extra factor of $1-R_\alpha$ which is missing from the Shuey expression (and, implicitly, from the Aki-Richards expression).

Turning now to B , we note that, to linear order in R_α , the factor in B^{θ_1} is $1+2R_\alpha$, while the factor in B^θ is simply 1. This suggests that the θ formulation should now be the most accurate, and this is sometimes observed, as noted above, but only in cases of minimal interest for exploration seismology. Elsewhere the reverse holds true. To explain this more complicated behavior it is necessary to derive an additional expression. Beginning again with the exact B , obtained from expressions in Appendix B, we assume that the key effects are independent of R_ρ (based on empirical observations), and set this quantity to zero. With no further approximation, we now have the new expressions

$$B^{\theta_1}(\text{nonlinear in } R_\beta; R_\rho = 0) = \frac{(R_\alpha - 8\gamma^2 R_\beta)(1+R_\alpha) + 16\gamma^3 R_\beta^2}{1-R_\alpha} \tag{10}$$

and

$$B^\theta = B^{\theta_1}(1-R_\alpha)^2. \tag{11}$$

These are similar to equation 7 (with $R_\rho = 0$) but now have an additional $\gamma^3 R_\beta^2$ term. (We note that carrying this procedure out on A_S does not yield an analogous higher-order term.) When either γ or R_β is small then this additional term will become negligible and

the $R_{pp}(\theta)$ expression will be more accurate, as predicted by equation 7. Consider however the simple case of $\gamma = 1/2$ and $R_\beta = R_\alpha$. Then equations 10 and 11 simplify to

$$B^{\theta_1} \approx -R_\alpha, \quad (12)$$

$$B^\theta \approx -R_\alpha(1-R_\alpha)^2. \quad (13)$$

For comparison if we apply $\gamma = 1/2$, $R_\rho = 0$, and $R_\beta = R_\alpha$ to the Shuey B we obtain $-R_\alpha$, so that for earth parameters in the vicinity of these conditions, it is once again the θ_1 formulation that will be more accurate, in accord with observations.

We have previously described the important role of R_β^2 corrections in the improvement of AVO theories (Ursenbach, 2004a,b). The necessity of invoking them here to explain near-offset R_{pp} behavior further illustrates their significance.

A SIMPLE IMPROVEMENT TO AVO THEORIES

The observations and explanations above confirm the following conclusion: The θ_1 expression is generally more accurate at low angles, while the θ expression is more accurate near the critical point. It is of course of interest at this point to investigate whether this understanding can translate into a new expression which includes the strengths of both. One way to accomplish this objective is to modify the original Aki-Richards expressions by multiplying each occurrence of $\sin \theta$ in the initial gradients by $1-R_\alpha$. This will retain the superior low-angle behavior, while still producing a critical angle at the correct location. We can implement and write this new expression as

$$R_{pp}^{\text{new}} = R_\rho + R_\alpha \left[1 + (1-R_\alpha)^2 \tan^2 \theta \right] - 4\gamma^2 (1-R_\alpha)^2 \sin^2 \theta (2R_\beta + R_\rho), \quad (14)$$

$$R_{ps}^{\text{new}} = -\gamma(1-R_\alpha) \tan \varphi \left[R_\rho + 2\gamma \cos(\theta - \varphi) (2R_\beta + R_\rho) \right]. \quad (15)$$

Because R_α now appears in the coefficients, these expressions are explicitly nonlinear. However we note that the original Aki-Richards expressions are already implicitly nonlinear, in that R_α is required in order to calculate θ . This value of R_α is typically obtained from the background α , given, for instance, by the velocity analysis. Therefore no additional information is required for these new expressions.

In Figures 6 and 7 below we plot these new expressions along with those previously considered. Figure 8 shows these quantities plotted over their full range, analogous to Figure 1. (These figures were created by a customized Reflectivity Explorer, for which the new theories are given by a magenta line. This modified Explorer is available in **REtest.html** in the software release accompanying this Research Report.) We make three observations regarding these figures: 1) The accuracy at low angles is similar to that of the θ_1 formulation. 2) The accuracy at the critical angle is similar to $R_{ps}(\theta)$, but not as good as $R_{pp}(\theta)$. 3) Because of the critical behavior, the low-angle accuracy extends over

a wider range than in the θ_1 formulation. To demonstrate this clearly, the plots extend to 50° rather than 30° as in Figures 3-6. These expressions should therefore be more efficacious than either of the previous formulations for precritical AVO analyses.

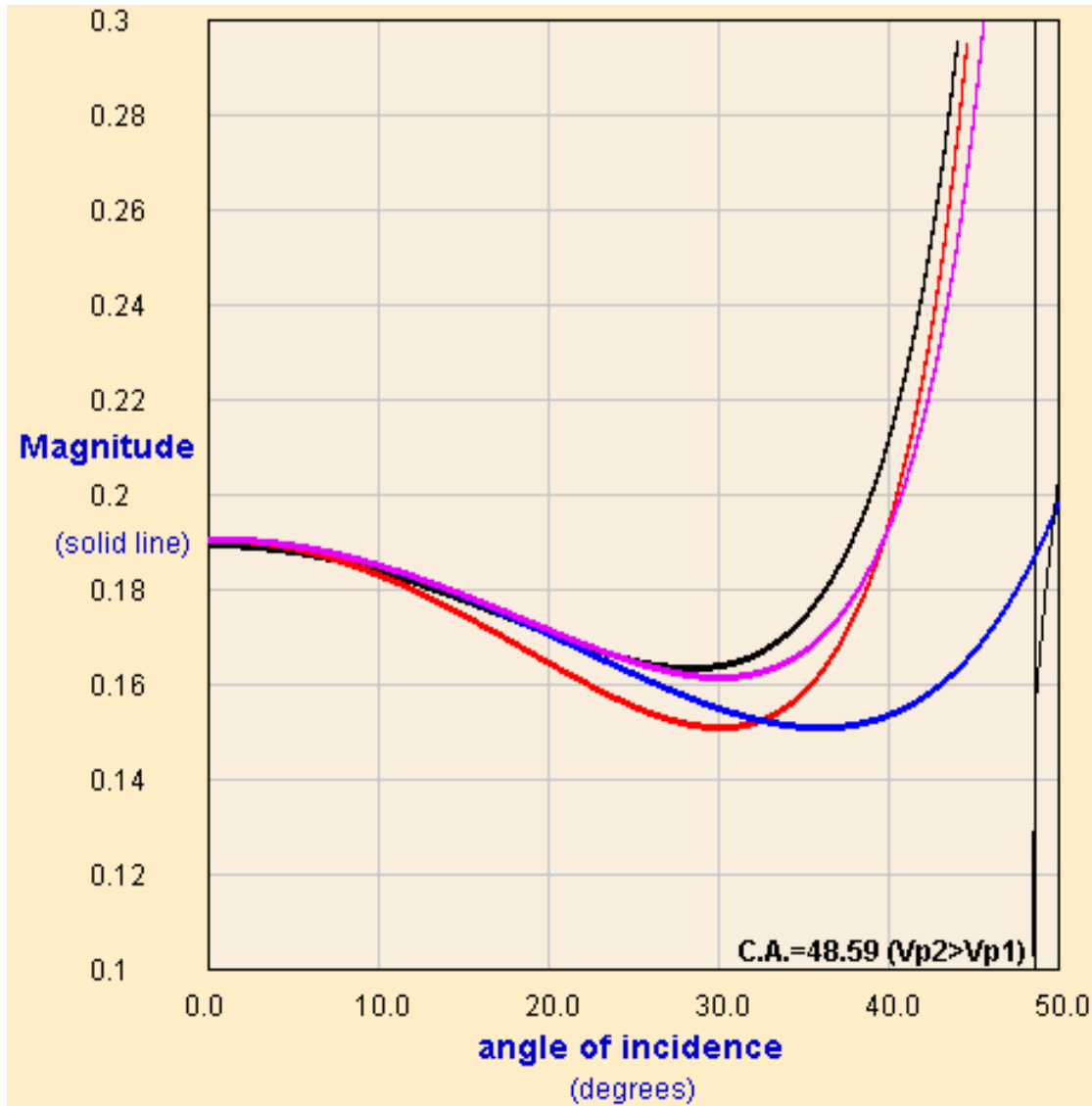


FIG. 6. A comparison of R_{PP} approximations, namely, $R_{PP}^{A-R}(\theta)$ (red), $R_{PP}^{A-R}(\theta_1)$ (blue), and the new method of equation 14 (magenta). The comparison is with the exact Zoeppritz expression (black). Compare with Figure 3.

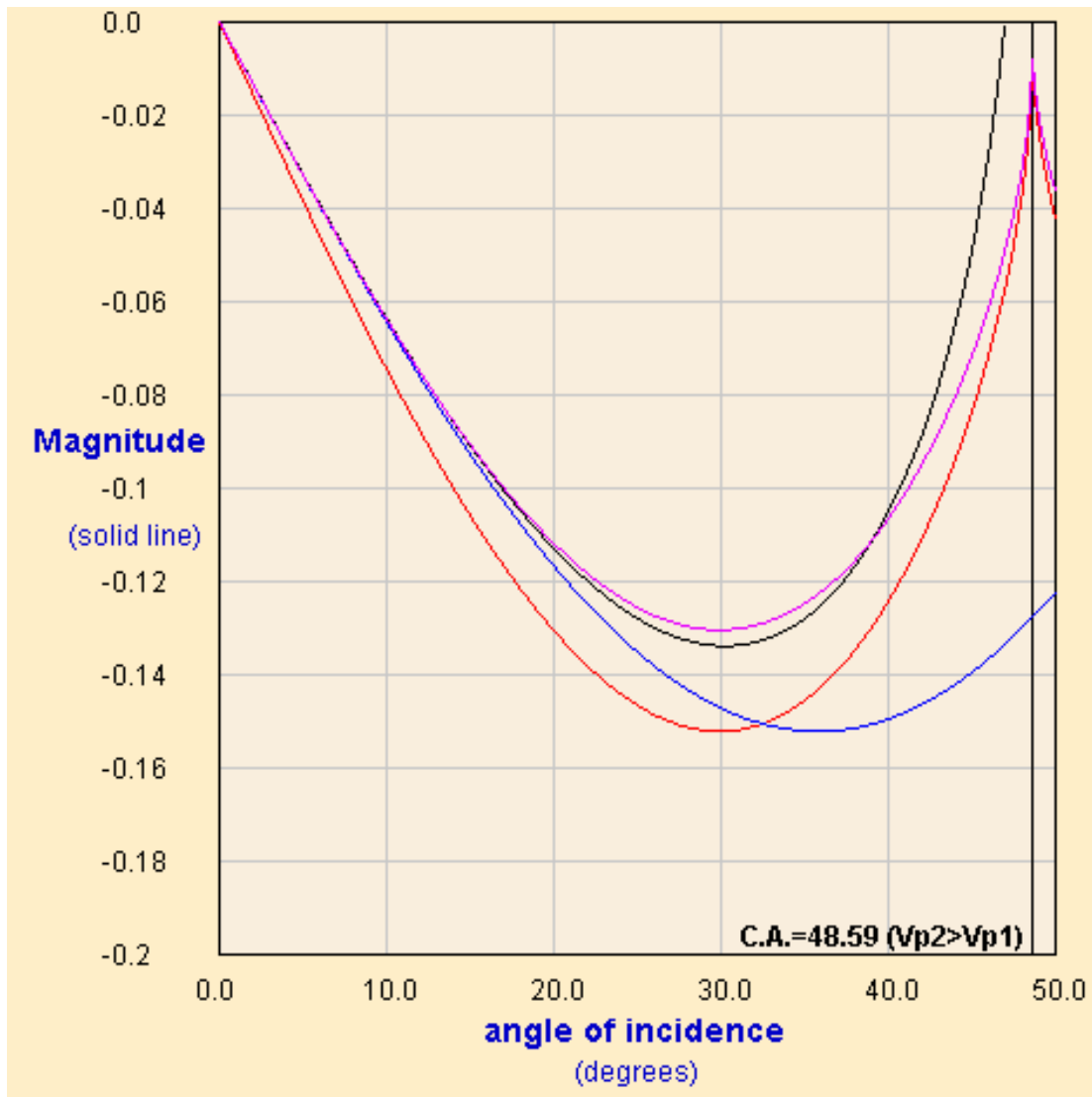


FIG. 7. A comparison of R_{PS} approximations, namely, $R_{PS}^{A-R}(\theta)$ (red), $R_{PS}^{A-R}(\theta_i)$ (blue), and the new method of equation 15 (magenta). The comparison is with the exact Zoeppritz expression (black). Compare with Figure 4.

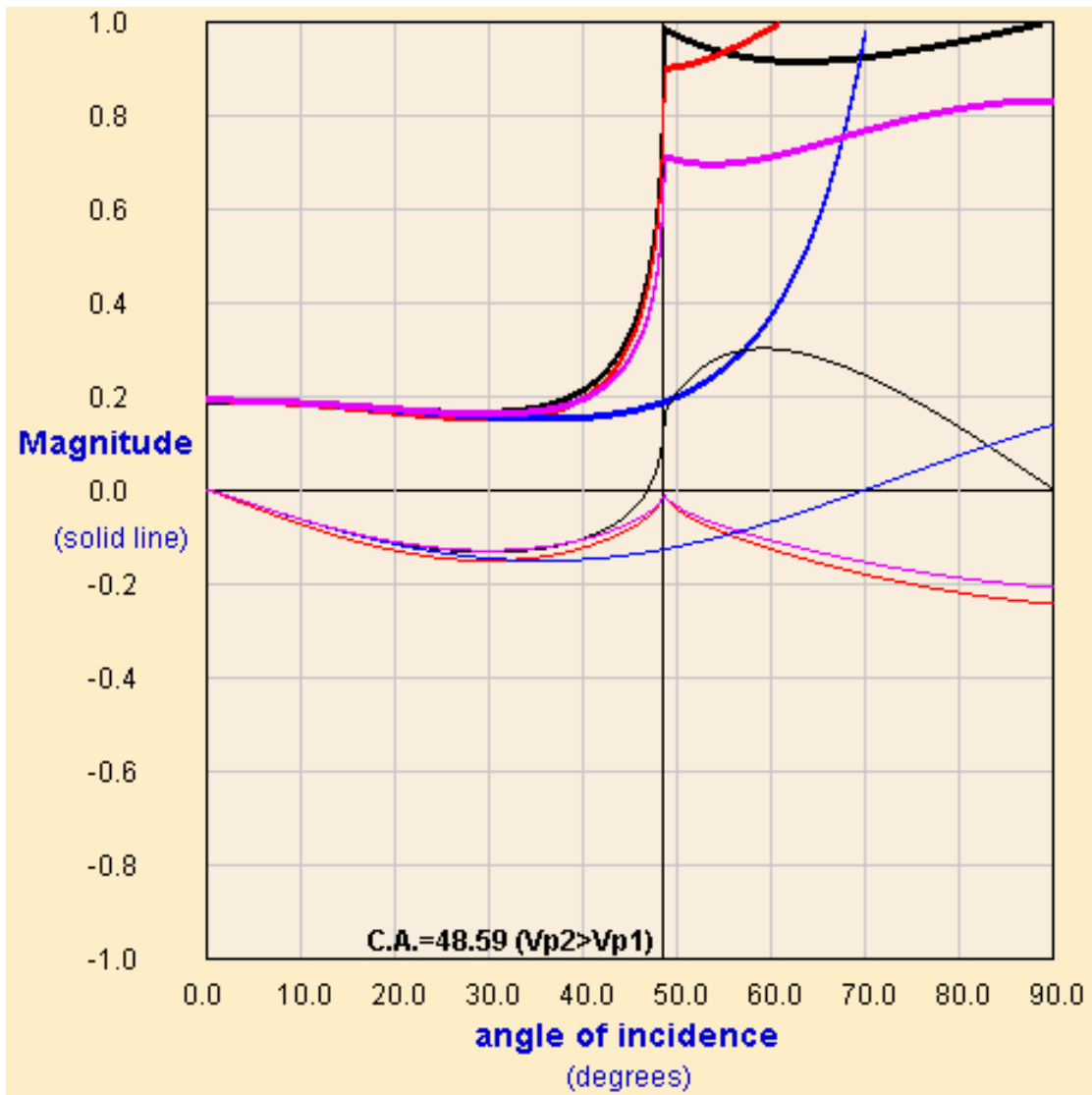


FIG. 8. A comparison of R_{PP} (thick lines) and R_{PS} (thin lines) approximations, namely, the θ -formulation (red), the θ_1 -formulation (blue), and the new method of equations 14 and 15 (magenta). The comparison is with the exact Zoeppritz expression (black). Compare with Figure 1.

DISCUSSION AND CONCLUSIONS

We have discussed the approximation of replacing θ by θ_1 in the Aki-Richards approximation. This worsens the approximation near the the critical angle, but, in the case of R_{PS} , improves it at low angles (0° - 30°). In the case of R_{PP} , the influence of R_β^2 terms in the exact gradient expression must be accounted for to explain the observation that $R_{PP}(\theta_1)$ is more accurate than $R_{PP}(\theta)$ for typical earth parameter combinations, but that $R_{PP}(\theta)$ is more accurate than $R_{PP}(\theta_1)$ for atypical combinations.

The Aki-Richards approximation is not the most commonly used AVO approximation. Three more commonly approximations are the two-term Shuey approximation (equation 4 with $C = 0$, the Smith-Gidlow approximation (Smith and Gidlow, 1987), and the Fatti approximation (Fatti et al., 1994), all of which are derived from the Aki-Richards approximation. Traditionally they are expressed in terms of θ . All of these methods, and especially their converted-wave analogues, would be benefited by the procedure used to obtain equations 14 and 15 from the Aki-Richards approximation.

REFERENCES

- Aki, K. and Richards, P. G., 1980, Quantitative Seismology: Theory and Methods: W.H. Freeman, 1980.
- Fatti, J. L., Smith, G. C., Vail, P. J., Strauss, P. J., and Levitt, P. R., 1994, Detection of gas in sandstone reservoirs using AVO analysis: A 3-D seismic case history using the Geostack technique: *Geophysics*, **59**, 1362-1376.
- Shuey, R. T., 1985, A simplification of the Zoeppritz equations: *Geophysics*, **50**, 609-614.
- Smith, G. C., and Gidlow, P. M., 1987, Weighted stacking for rock property estimation and detection of gas: *Geophys. Prospecting*, **35**, 993-1014.
- Ursenbach, C., 2004a, Three new approximations for estimation of R_j from AVO: CREWES Research Report, **16**.
- Ursenbach, C., 2004b, A non-linear, three-parameter AVO method that can be solved non-iteratively: CREWES Research Report, **16**.

APPENDIX A: COMPLEX SUPERCritical TRANSMISSION ANGLE

By Snell's law, $\sin \theta_2 = (\alpha_2 / \alpha_1) \sin \theta_1$. If $\alpha_2 > \alpha_1$, then a critical angle is located at $\sin \theta_1 = \alpha_1 / \alpha_2$, which implies $\sin \theta_2 = 1$. Beyond the critical angle, $\sin \theta_2 > 1$, i.e., it is positive real, but greater than unity. Then $\cos \theta_2 = \sqrt{1 - \sin^2 \theta_2} = \sqrt{-|1 - \sin^2 \theta_2|} = i\sqrt{|1 - \sin^2 \theta_2|}$, i.e., it is positive imaginary.

These two conditions place constraints on the form of θ_2 . Let us assume that it is in general complex, i.e., $\theta_2 = x + iy$, $x, y \in R$. Then

$$\begin{aligned} \sin \theta_2 &= \sin(x + iy) \\ &= \sin x \cos(iy) + \cos x \sin(iy) \\ &= \sin x \cosh y + i \cos x \sinh y \\ \cos \theta_2 &= \cos(x + iy) \\ &= \cos x \cos(iy) - \sin x \sin(iy) \\ &= \cos x \cosh y - i \sin x \sinh y. \end{aligned}$$

Applying the previously obtained conditions we have

$$\begin{aligned} \sin x \cosh y &> 1 \\ \cos x \sinh y &= 0 \\ \cos x \cosh y &= 0 \\ \sin x \sinh y &< 0. \end{aligned}$$

These conditions can only be simultaneously satisfied if

$$x = \frac{\pi}{2} + 2n\pi, \quad n \in I.$$

This implies that

$$\begin{aligned} \sin \theta_2 &= \cosh y \\ y &= -\cosh^{-1}(\sin \theta_2). \end{aligned}$$

(The \cosh^{-1} operation is double-valued, which we indicate by the notation $\pm \cosh^{-1}$.) At the critical angle $n = 0$, so we can then write

$$\theta_2 = \frac{\pi}{2} - i \cosh^{-1} \left(\frac{\alpha_2}{\alpha_1} \sin \theta_1 \right).$$

This result also holds formally for precritical angles, but in that case the \cosh^{-1} operation yields imaginary results.

APPENDIX B: ZOEPPRITZ COEFFICIENTS GIVEN IN REFLECTIVITIES

Aki and Richards (1980, pp 149-151) give expressions for the Zoeppritz coefficients. Below we give similar expressions, but in terms of reflectivities (defined in equation 1) rather than in terms of earth parameters. We use the same notation for angles as Aki and Richards, namely,

$$\begin{aligned} i_1 &= \text{incident P-wave angle } (\theta_1) \\ i_2 &= \text{transmitted P-wave angle } (\theta_2) \\ j_1 &= \text{reflected converted-wave angle } (\varphi_1) \\ j_2 &= \text{transmitted converted-wave angle } (\varphi_2) \end{aligned}$$

The expressions for $R_{PP}(R_\alpha, R_\beta, R_\rho, \gamma; \theta_1)$ and $R_{PS}(R_\alpha, R_\beta, R_\rho, \gamma; \theta_1)$ are as follows:

$$R_{PP} = \frac{(b \cot i_1 - c \cot i_2)F - (a + d \cot i_1 \cot j_2)H}{D}$$

$$R_{PS} = -2 \frac{\cos i_1}{\sin j_1} \frac{ab + cd \cot i_2 \cot j_2}{D}$$

$$D = EF + GH$$

$$E = b \cot i_1 + c \cot i_2$$

$$F = b \cot j_1 + c \cot j_2$$

$$G = a - d \cot i_1 \cot j_2$$

$$H = a - d \cot i_2 \cot j_1$$

$$a = (1 + R_\rho)(1 - 2 \sin^2 j_2) - (1 - R_\rho)(1 - 2 \sin^2 j_1)$$

$$b = (1 + R_\rho)(1 - 2 \sin^2 j_2) + 2(1 - R_\rho) \sin^2 j_1$$

$$c = (1 - R_\rho)(1 - 2 \sin^2 j_1) + 2(1 + R_\rho) \sin^2 j_2$$

$$d = 2(1 + R_\rho) \sin^2 j_2 - 2(1 - R_\rho) \sin^2 j_1$$

$$\cot x = \frac{\sqrt{1 - \sin^2 x}}{\sin x}$$

$$\sin i_2 = \frac{1 + R_\alpha}{1 - R_\alpha} \sin i_1$$

$$\sin j_1 = \gamma \frac{1 - R_\beta}{1 - R_\alpha} \sin i_1$$

$$\sin j_2 = \gamma \frac{1 + R_\beta}{1 - R_\alpha} \sin i_1$$

The above expressions may be programmed into a symbolic language (such as MAPLE or MATHEMATICA) in the order given. For a computing language (such as FORTRAN or C) they are programmed in the reverse order.

APPENDIX C: EXACT EXPRESSIONS FOR INTERCEPT AND GRADIENTS

The R_{PP} intercept and gradient, A and B , and the R_{PS} gradient, A_S , can be obtained exactly in terms of reflectivities from the expressions in Appendix B. For completeness these quantities are given here.

$$A = \frac{R_\alpha + R_\rho}{1 + R_\alpha R_\rho}$$

$$B = [4\gamma^3(1 - R_\rho)\bar{R}_\mu^2 - 4\gamma^2(1 + R_\alpha)(1 - R_\rho^2)\bar{R}_\mu - \gamma(1 + R_\alpha)^2(1 - R_\beta^2)(1 + R_\rho)R_\rho^2 + \dots \\ + (1 + R_\alpha)(1 - R_\rho^2)(1 + R_\beta R_\rho)R_\alpha] / [(1 + R_\alpha R_\rho)^2(1 + R_\beta R_\rho)(1 - R_\alpha)]$$

$$A_S = -\frac{2\gamma(1 - R_\rho)\bar{R}_\mu + (1 + R_\alpha)(1 + R_\beta)(1 + R_\rho)R_\rho}{(1 + R_\alpha R_\rho)(1 + R_\beta R_\rho)}$$

Here we have defined

$$\bar{R}_\mu \equiv 2R_\beta + R_\rho + R_\beta^2 R_\rho$$

(Note that we normally define $\mu \equiv \rho\beta^2$, which leads to

$$R_\mu \equiv (2R_\beta + R_\rho + R_\beta^2 R_\rho) / (1 + R_\beta^2 + R_\beta R_\rho) = \bar{R}_\mu / (1 + R_\beta^2 + R_\beta R_\rho).$$

We use the overbar notation to indicate that the quantities R_μ and \bar{R}_μ are similar but not identical.)

APPENDIX D: EXACT RELATION BETWEEN SINES OF INCIDENT AND AVERAGE ANGLES

We derive the relation between $\sin \theta$ and $\sin \theta_1$, beginning with the definition of $\sin \theta$:

$$\sin \theta = \sin \frac{\theta_1 + \theta_2}{2} = \sin \frac{\theta_1}{2} \cos \frac{\theta_2}{2} + \cos \frac{\theta_1}{2} \sin \frac{\theta_2}{2},$$

$$\sin \theta = \sqrt{\frac{1 - \cos \theta_1}{2}} \sqrt{\frac{1 + \cos \theta_2}{2}} + \sqrt{\frac{1 + \cos \theta_1}{2}} \sqrt{\frac{1 - \cos \theta_2}{2}}.$$

Squaring this yields

$$\sin^2 \theta = \frac{1}{2} [1 - \cos \theta_1 \cos \theta_2 + \sin \theta_1 \sin \theta_2],$$

which may be recast as

$$2 \sin^2 \theta - 1 - \frac{1 + R_\alpha}{1 - R_\alpha} \sin^2 \theta_1 = -\sqrt{1 - \sin^2 \theta_1} \sqrt{1 - \left(\frac{1 + R_\alpha}{1 - R_\alpha}\right)^2 \sin^2 \theta_1}.$$

Squaring again and simplifying gives

$$\left[\frac{1}{(1 - R_\alpha)^2} \cos^2 \theta + \left(\frac{R_\alpha}{1 - R_\alpha}\right)^2 \sin^2 \theta \right] \sin^2 \theta_1 = \sin^2 \theta \cos^2 \theta$$

which may be rearranged to

$$\sin^2 \theta_1 = \sin^2 \theta \frac{(1 - R_\alpha)^2}{1 + R_\alpha^2 \tan^2 \theta}.$$

Equation 9 then follows from the positive square root.